A MODIFIED GOODNESS-OF-FIT MEASUREMENT FOR RADAR CLUTTER AMPLITUDE STATISTICS

Liang Li, Lingjiang Kong[*]**, and Xiaobo Yang**

School of Electronic Engineering, University of Electronic Science and Technology of China, Chengdu, China

Abstract—This paper addresses the application of measurement on goodness-of-fit (GoF) for amplitudes of radar clutter sample data against reference/theoretic parameterized probability density function (PDF). In general, various existing methods for this problem highly depend on empirical PDF parameters. This makes GoF assessments with these methods less perceivable and their accuracies are hard to control. A new method based on chi-squared type of measurement is proposed to overcome these difficulties. This method evaluates GoF by estimating the distance between the true PDF of the clutter data amplitude and the reference PDF. Hence the distance is statistically approximately independent with empirical PDF parameters. The new method has higher accuracy and symmetric property. It is especially useful for GoF comparison over multiple radar clutter data sets.

1. INTRODUCTION

Sea-clutter and ground-clutter play an important role in radar signal analysis, modeling and processing. Clutter amplitude distribution is one of the well-known statistical characteristics in clutter study. Existing works on modeling and fitting clutter amplitude distribution include Gaussian based Rayleigh distribution and Compound-Gaussian distributions such as Weibull, Log-normal, and K, etc. [1–5]. Based on these studies, clutter amplitude distribution is further incorporated into design and analysis of constant false alarm ratio (CFAR) system [6, 7], small target detection [8], target recognition [9], and so on.

Traditional studies on clutter amplitude generally consists of two parts — fitting a data set with a specific model and calculating a goodness-of-fit for the fitting result.

* Corresponding author: Lingjiang Kong (lingjiang.kong@gmail.com).

In the fitting process, parameters for a determined statistical model are generally estimated by the Method of Moments (MoM) [2, 8, 10], the Method of Fractural Moments (MoFM) [4, 10] or Maximum Likelihood estimation (MLE) [7, 10]. In [10], Balleri and Nehorai demonstrated that for the sea-clutter data distribution model, MLE overwhelms others and achieves the asymptotically efficient property.

After the parameters are determined by the fitting process, one computes goodness-of-fit (GoF) to measure how the model accords with the clutter sample data. To compute GoF, there are many methods such as visual inspection on PDF plot, mean square error (MSE) of PDF, MSE of the of logarithm PDF, Pearson's chi-squared test statistic, Hellinger distance, G-test statistic, Kullback-Leibler divergence, etc. [2, 4, 8, 11–15]. Among these methods, Pearson's chi-squared test, Hellinger distance and G-test belong to the chi-squared type of statistics, and they have asymptotic approximation with likelihood ratio statistic [16].

Traditional GoF measurements from different sample data sets are difficult to compare with each other if sample number or empirical PDF parameters are not equal. In existing studies on clutter amplitude, GoF are generally treated as a subordinate procedure. Criteria for fitting dose not always equivalent with the condition that yield for the best GoF.

This paper proposes a new measurement for both fitting and GoF. The measurement is defined as a distance between true PDF and reference PDF, which is statistically independent of sample data number and approximately insensitive to parameters in estimating empirical PDF. In addition, as a cost function in the fitting process, the measurement is asymptotically approximate to MLE. As a GoF, it is a symmetric measurement, has a non-negative expectation and diminishes when true PDF and reference PDF are identical, namely zero distance.

2. EXISTING CHI-SQUARED TYPE METHODS AND THEIR LIMITATIONS

The GoF is quantified by a distance, which is traditionally calculated from an empirical PDF of the radar clutter data set and a reference PDF. Denote the true PDF that sample data follows as PDF_d and the reference PDF as PDF_r.

The estimation of PDF_d is acquired via histogram, where the amplitude is divided into m successive inlaid cells from 0 to a finite value and a series of observed frequencies are acquired from a set of

sampled data, denoted as $\mathbf{O} = [O_1, \ldots, O_m]$. Referenced frequencies are calculated according to the PDF_r and the same data number and cell divisions with $\mathbf{O}$ and denoted as $\mathbf{R} = [R_1, \ldots, R_m]$. Since Radar clutter amplitude data samples are typically mustered in a finite range, the range of amplitude is chosen so that the sum of $\mathbf{O}$ is close to the sample data number in practice.

Let x be the amplitude coordinate. Suppose PDF_r and PDF_d are expressed as $\text{pdf}_r(x)$ and $\text{pdf}_d(x)$ over x respectively. The functions $\text{pdf}_r(x)$ and $\text{pdf}_d(x)$ are assumed to be continuous and smooth. Given histogram cells are sufficient small, we have the following

$$\begin{cases} R_i \approx n \cdot cs_i \cdot \text{pdf}_r(x_i), \\ E[O_i] \approx n \cdot cs_i \cdot \text{pdf}_d(x_i), \end{cases} \tag{1}$$

where $E[\cdot]$ denotes the statistical expectation, n the number of data sample, and cs_i the histogram cell-size for the i-th cell. In addition, O_i follows a binomial distribution as $B(n, cs_i \cdot \text{pdf}_d(x_i))$ [17]. For large n and small $cs_i \cdot \text{pdf}_d(x_i)$, Poisson distribution with parameter $n \cdot cs_i \cdot \text{pdf}_d(x_i)$ can be used as an approximation [18]. We assume large n and small cs_i in the following sections therefore O_i approximately follows a Poisson distribution.

We define the chi-squared type measurement χ^2 to be

$$\chi^2 = \sum_{i=1}^{m} \eta(R_i, O_i), \tag{2}$$

where $\eta_i = \eta(R_i, O_i)$ is individual calculation for a pair (R_i, O_i) in a single cell and we designate $\mu(\cdot)$ as a *cell function*. In the following, χ^2_P, χ^2_G, χ^2_H and χ^2_M are chi-squared type of measurements with different *cell functions*. Ideally, χ^2 follows a non-central chi-squared distribution and when PDF_r and PDF_d are equal (null hypothesis), the non-central parameter is expected to be zero.

In [2], Pearson's chi-squared test statistic is

$$\chi^2_P = \sum_{i=1}^{m} \eta_{Pi} = \sum_{i=1}^{m} \frac{(R_i - O_i)^2}{R_i}. \tag{3}$$

Performance of χ^2_P, especially under null hypothesis, depends on extent of approximation of η_{Pi} towards chi-squared distribution. Another chi-squared test statistic known as G-test statistic is proposed as the replacement of Pearson's chi-squared test statistic for higher accuracy, defined as

$$\chi^2_G = \sum_{i=1}^{m} \eta_{Gi} = \sum_{i=1}^{m} 2O_i \ln \frac{O_i}{R_i}. \tag{4}$$

In [16], Koehler and Larntz proved that χ_P^2 and χ_G^2 are asymptotically equal. Compared with Pearson's chi-squared test statistic, G-test statistic has better approximation to the theoretical chi-squared distribution. There is less bias when χ_G^2 is used in replacement of χ_P^2.

From (3) and (4), χ_P^2 and χ_G^2 depend on the empirical PDF parameters such as, the sample number, the histogram cell-size and the range of the PDF.

In addition, (3) and (4) are asymmetric measurements in compare with Hellinger distance [19], denoted as χ_H^2. In [19], Cha uses 'addition' method to transform asymmetric distance into symmetric one. It transforms χ_P^2 and χ_G^2 into a symmetric chi-squared and Jeffrey's statistic respectively. However, these two modifications contain caveats of either divide by zero or log of zero in implementation.

3. PROPOSED METHOD

Based on existing chi-squared type measurements, we define a new symmetric measurement as

$$\chi_M^2 = \sum_{i=1}^{m} \eta_{M_i} = \sum_{i=1}^{m} \left(f_a(R_i) - f_b(O_i) \right)^2, \tag{5}$$

where $f_a(\cdot)$ and $f_b(\cdot)$ are defined in (8). We have

$$
\begin{aligned}
E[\chi_M^2] &= \sum_{i=1}^{m} E\left[f_a(R_i)^2 + f_b(O_i)^2 - 2f_b(O_i)f_a(R_i) \right] \\
&= \sum_{i=1}^{m} f_a(R_i)^2 + \text{var}(f_b(O_i)) + E[f_b(O_i)]^2 - 2f_a(E_i)E[f_b(O_i)] \\
&= \sum_{i=1}^{m} \text{var}(f_b(O_i)) + \left(f_a(R_i) - E[f_b(O_i)] \right)^2,
\end{aligned}
\tag{6}
$$

where $\text{var}(\cdot)$ is the variance operator.

It is desirable that the expectation of the measurement gets a constant minimum under null hypothesis. This is equivalent to the following conditions

$$\begin{cases} f_a\left(R_i|_{R_i = E[O_i]} \right) - E[f_b(O_i)] = 0, \\ \text{var}(f_b(O_i)) = \text{constant}. \end{cases} \tag{7}$$

To meet the requirements, we define

$$\begin{cases} f_a(R_i) = E\left[f_{\text{vst\_opt}}(q|_{\lambda=R_i}) \right], \\ f_b(O_i) = f_{\text{vst\_opt}}(O_i), \end{cases} \tag{8}$$

where q is a Poisson random variable with parameter λ, $f_{\text{vst\_opt}}(\cdot)$ is the optimized variable stabilizing transform (VST) [20]. For a Poisson random variable v with parameter λ, $\text{var}(f_{\text{vst\_opt}}(v)) \approx 1$ for $\lambda > 4$. As addressed in [21], it is impossible to simultaneously achieve good stabilization for all parameter values. Error in measurement caused by this imperfection is inevitable. The optimized VST is a proper trade off between performance and simplicity.

$$f_{\text{vst\_opt}}(v) = \frac{2(v + 3/8 + \sqrt{3}/12)}{\sqrt{v + 3/8 + \sqrt{3}/6}}. \tag{9}$$

Compared with many other VSTs such as Anscombe, Freeman & Tukey, (10) has better approximation to constant variation [18].

Substituting (8) into (5), we have a modified measurement as

$$\chi_M^2 = \sum_{i=1}^{m} \eta_{Mi} = \sum_{i=1}^{m} \left(E[f_{\text{vst\_opt}}(q|_{\lambda=R_i})] - f_{\text{vst\_opt}}(O_i) \right)^2. \tag{10}$$

Measurement χ_M^2 is also an chi-squared statistics similar to χ_P^2. From [22], χ_P^2 follows a non-central chi-squared distribution with $(m - 1 - p)$ degrees of freedom, where p is a value between 0 and the number of independent parameters of the PDF$_r$. For large m, we set $p = 0$ for simplicity with ignorable error and assume χ_M^2 follows a non-central chi-squared distribution with $(m - 1)$ degrees of freedom. Then its mean and variance can be inferred from (6) as

$$\begin{cases} E[\chi_M^2] \approx m - 1 + \sum_{i=1}^{m} \left(E[f_{\text{vst\_opt}}(q|_{\lambda=R_i})] - E[f_{\text{vst\_opt}}(O_i)] \right)^2, \\ \text{var}(\chi_M^2) \approx 4E[\chi_M^2] - 2(m - 1). \end{cases} \tag{11}$$

We make a preliminary comparison among three *cell functions*, η_P, η_G and η_M in (3)–(5). Let a cell has a reference frequency of λ_r and a Poisson distributed observed frequency with parameter λ_d.

In Figures 1 and 2, the expectations for the three *cell functions* under the condition of unequal (λ_r, λ_d) pairs and their swapped value alternatives are represented by solid lines and dotted lines. Specifically, we call the measurements for $(\lambda_d = 8 + \Delta\lambda, \lambda_r = 8 - \Delta\lambda)$ and $(\lambda_d = 8 - \Delta\lambda, \lambda_r = 8 + \Delta\lambda)$ as a *combination*. *Combinations* for $E[\eta_P]$, $E[\eta_G]$ and $E[\eta_M]$ are distinguished by circle marker and asterisk marker and no marker, respectively.

Figure 1 shows that, η_M is the only symmetric measurement among the three. For the solid line and the dotted line for $E[\eta_M]$ is superposed, while *combinations* for both $E[\eta_P]$ and $E[\eta_G]$ are separated.
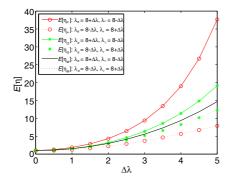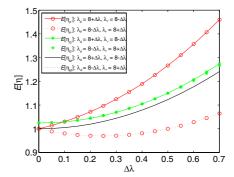
Figure 1. Expectation of η for unequal (λ_r, λ_d) pairs.

Figure 2. Expectation of η for unequal (λ_r, λ_d) pairs for small $\Delta\lambda$.

Figure 2 shows $E[\eta_G]$ is less asymmetric than $E[\eta_M]$, when the difference between λ_r and λ_d is relatively small. When λ_r and λ_d are equal, $E[\eta_G]$ is biased from 1 unlike $E[\eta_P]$ and $E[\eta_M]$.

As sums of independent individual measurements, χ_P^2, χ_G^2 and χ_M^2 inherit characteristics form their *cell functions*. Therefore χ_M^2 is a more accurate symmetric measurement.

Define

$$\begin{cases} D_P = \left[\chi_P^2 - (m-1)\right]/n, \\ D_G = \left[\chi_G^2 - (m-1)\right]/n, \\ D_M = \left[\chi_M^2 - (m-1)\right]/n, \end{cases} \tag{12}$$

where n is the number of data sample. Provided that χ_M^2 approximately follows a non-central chi-squared distribution with $(m-1)$ degrees of freedom, D_M is a shifted and scaled version of a non-central chi-squared variable. Refer to (11), it has

$$\begin{cases} E[D_M] \approx \dfrac{1}{n} \sum_{i=1}^{m} \left(E[f_{\text{vst\_opt}}(q|_{\lambda=R_i})] - E[f_{\text{vst\_opt}}(O_i)]\right)^2, \\ \text{var}[D_M] \approx \dfrac{1}{n^2}\left(4nE[D_M] + 2(m-1)\right). \end{cases} \tag{13}$$

We now prove that $E[D_M]$ is approximately independent to n, cs and insensitive to the amplitude range u.

From (9), $f_{\text{vst\_opt}}(v) \approx 2\sqrt{v}$, therefore

$$\begin{cases} E\left[f_{\text{vst\_opt}}(u|_{\lambda=R_i})\right] \approx E\left[2\sqrt{q|_{\lambda=R_i}}\right], \\ E\left[f_{\text{vst\_opt}}(O_i)\right] \approx E\left[2\sqrt{O_i}\right], \end{cases} \tag{14}$$

and

$$\begin{cases} E\left[\sqrt{q|_{\lambda=R_i}}\right] \propto \sqrt{n \cdot cs_i \cdot \text{pdf}_r(x_i)}, \\ E\left[\sqrt{O_i}\right] \propto \sqrt{n \cdot cs_i \cdot \text{pdf}_d(x_i)}. \end{cases} \quad (15)$$

Substituting (15) into (14), we have

$$(E[f_{\text{vst\_opt}}(q|_{\lambda=R_i})] - E[f_{\text{vst\_opt}}(O_i)])^2$$
$$\propto n \cdot cs_i \left(\sqrt{\text{pdf}_r(x_i)} - \sqrt{\text{pdf}_d(x_i)}\right)^2 \quad (16)$$

Substituting (16) into (13), n is canceled out. We have

$$E[D_M] \propto \sum_{i=1}^{m} cs_i \left(\sqrt{\text{pdf}_r(x_i)} - \sqrt{\text{pdf}_d(x_i)}\right)^2 \quad (17)$$

The summation can be approximated by integration

$$\sum_{i=1}^{m} cs_i \left(\sqrt{\text{pdf}_r(x_i)} - \sqrt{\text{pdf}_d(x_i)}\right)^2 \approx \int_0^u \left(\sqrt{\text{pdf}_r(x)} - \sqrt{\text{pdf}_d(x)}\right)^2 dx, \quad (18)$$

where amplitude range $u = x_m + cs_m/2$. Parameter cs_i and m also vanish. For Radar clutter data, the amplitude PDF is typically monotonous decreasing with x. For sufficient large u, it holds for

$$\int_0^u \left(\sqrt{\text{pdf}_r(x)} - \sqrt{\text{pdf}_d(x)}\right)^2 dx \approx \int_0^\infty \left(\sqrt{\text{pdf}_r(x)} - \sqrt{\text{pdf}_d(x)}\right)^2 dx. \quad (19)$$

The integration in (18) is insensitive to u, as long as u is large and so dose $E[D_M]$.

4. NUMERICAL EXPERIMENTS

We present two simulations and an experiment. The first simulation presents the performance of the proposed method. The second one compares the estimating performance of the proposed method with that of traditional methods. The last experiment demonstrates an application of the proposed method on a real radar data set.

In the first two simulations, we use a Log-normal and a K distribution, defined as (20), for PDF_d and PDF_r. The default configurations are listed in Table 1. The parameters for distributions are chosen so that they represent typical amplitude PDF for non-Gaussian clutter with long tails [23].

$$\begin{cases} f_{\text{Log-normal}}(x, \mu, \sigma) = \frac{1}{x\sigma\sqrt{2\pi}} \exp\frac{-(\ln x - \mu)^2}{2\sigma^2}, \\ f_{\text{K}}(x, b, v) = \frac{2b}{\Gamma}\left(\frac{bx}{2}\right)^v K_{v-1}(bx). \end{cases} \quad (20)$$

Table 1. Default configurations for the simulations.

	value	symbol
Scale parameter	0.5	μ
Shape parameter	0.7	σ
K parameter 1	1	b
K parameter 2	5	v
Sample number	100000	n
Cell size	0.02	cs
Maximum histogram range	20	u

Table 2. Distance vs. shape parameter.

	D_P	D_G	D_M
$\sigma_r = 0.7 - 0.005, \sigma_d = 0.7 + 0.005$	0.000215	0.000471	0.000410
$\sigma_r = 0.7 + 0.005, \sigma_d = 0.7 - 0.005$	0.000646	0.000471	0.000409
$\sigma_r = 0.7 - 0.01, \sigma_d = 0.7 + 0.01$	0.00117	0.00164	0.00161
$\sigma_r = 0.7 + 0.01, \sigma_d = 0.7 - 0.01$	0.00218	0.00171	0.00161
$\sigma_r = 0.7 - 0.02, \sigma_d = 0.7 + 0.02$	0.00521	0.00630	0.00645
$\sigma_r = 0.7 + 0.02, \sigma_d = 0.7 - 0.02$	0.00846	0.00682	0.00646
$\sigma_r = 0.7 - 0.03, \sigma_d = 0.7 + 0.03$	0.0118	0.0140	0.0146
$\sigma_r = 0.7 + 0.03, \sigma_d = 0.7 - 0.03$	0.0199	0.0157	0.0146

Results of the first simulation are shown in Table 2. They are averaged distances from 1000 independent experiments. Denote the shape parameters for PDF_d and PDF_r by σ_d and σ_r respectively. σ_d and σ_r in Table 2 are centralized in 0.7, and their separation is gradually increased to produce a series of mismatch situations.

The property of symmetry measurement is shown by D_M. D_M increases monotony with difference between σ_r and σ_d, and insensitive to whether the pair swaps value. On the opposite, asymmetric measurement produces significantly different results on pairs of swapped shape parameters. This is clearly demonstrated by D_P and D_G. It is also shown that asymmetry produces less bias on D_M when σ_r and σ_d are closer. For all simulations, D_G is less asymmetric than D_P, as expected. Despite of asymmetry, D_G is greater than D_M when the difference between the shape parameters is approximately smaller than 0.02, as the result of bias in D_G.

For D_M, performance of normalization against the number of data

sample and the histogram cell-size are demonstrated by Figures 3 and 4. In Figures 3 and 4, each marker represents an independent experiment. The solid lines and dotted lines string those results that have same shape parameter configurations. Fluctuations on each line are result of stochastic nature of empirical PDF.

In Figure 3, the fluctuations on all four lines decrease as n gets larger. Except for the fluctuations, D_M with the same shape parameter configuration remains largely constant with respect to a large range of sample data number. This supports the idea that D_M is approximately independent to the sample data number. Besides, results in the two dotted lines are closely enlaced. This further suggests that D_M is a symmetric measurement.
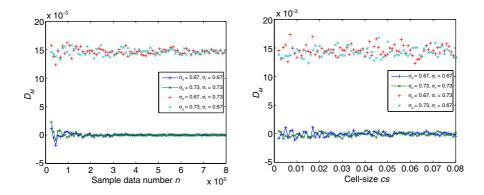

Figure 3. D_M vs. sample data number n.
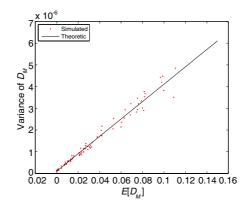
Figure 4. D_M vs. cell-size cs.

Figure 5. Variance of D_M vs. $E[D_M]$.

Figure 4 shows the independence of D_M from the histogram cell-size cs, in both match and mismatch of empirical and reference PDF conditions, as a result of the proposed normalization operation.

In Figure 4, D_M remains a constant for a large range of the cell-size except some fluctuations. Recall for (13), the fluctuation in D_M consists of two components. One is proportional to the expectation of D_M, and another is proportional to $(m-1)$.

In case that shape parameters in PDF_d and PDF_r are unequal, D_M has positive mean value, and fluctuation is dominated by the former component. In case that shape parameters in PDF_d and PDF_r are equal, that fluctuation is dominated by the later component. The two solid line stringed results illustrate the trend that fluctuation reduces as cell-size increases.

The relation within variance of D_M and the expectation of D_M, as expressed in (13), is verified by a simulation and shown in Figure 5.

One hundred different shape parameter pairs are randomly chosen from 0.6 to 0.8 for PDF_r and PDF_d. For each PDF_r and PDF_d pair, $E[D_M]$ and $\text{var}(D_M)$ are drawn from 200 independent experiments.
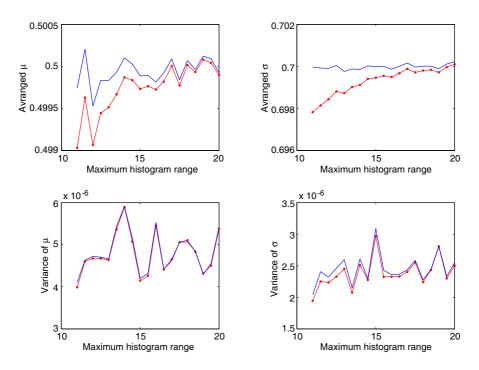

Figure 6. Parameter estimation results for Log-normal distribution solid line for the proposed method, line with dot marker for ML.

The results are plotted as dots in Figure 4. Comparing with theoretic ones in (13), the simulated result complies with the theory.

This implies the variance of D_M can be predicted from D_M through (13). The variance of D_M is generally increasing along with the expectation of D_M. The scatter pattern in Figure 5 also suggests the larger uncertainty lies in this relationship. This is a practically useful property of D_M, because the higher accuracy of D_M is expected when it is close to 0 to guarantee the faithfulness and the greater sensitivity of the measurement.

In the second simulation, we use a Log-normal distribution and a K distribution to compare parameter estimating performances of the proposed method and the traditional ones. The parameters of two distributed data sets are estimated by the Maximum Likelihood (ML) estimator and the Method of Moments (MoM) [24], respectively. For the new method, parameters are obtained by minimizing D_M.

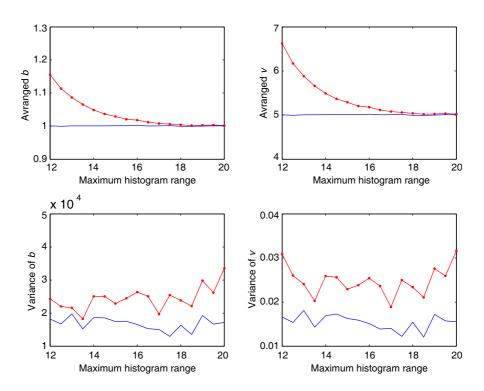We consider saturation in the simulation, i.e., in the data set, the

Figure 7. Parameter estimation results for K distribution solid line for the proposed method, line with dot marker for MoM.
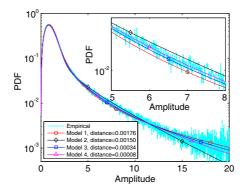
Figure 8. Application of the proposed method on real data.

amplitude of all samples are upper bounded to the maximum amplitude u. In the simulation, average proportions of saturated samples in the data set for the both distributions are monotonously decreasing from 0.4% to 0.02% with respect to u. Figures 6 and 7 suggest that saturation causes significant bias on the ML estimator and MoM. There is no observable bias on the proposed method for all u. For larger u, where saturation is ignorable to ML estimator and MoM, comparison of estimating accuracies can be made, approximately. The variances of the estimated parameters by the proposed method for all u are similar to those made by ML estimator and smaller than MoM's in their near saturation free region. This suggests that the proposed method has a similar estimating accuracy to the ideal ML estimator despite of certain amount of saturation.

In the last experiment, we use an IPIX's Grimsby 1998 sea clutter data to demonstrate the application of the proposed method on a real data set, i.e., file 155 (19980227_214328_antstep.cdf) 9 meter range resolution HH polarization [25]. The empirical PDF acquired from the data set is shown in Figure 8. We use 4 different Compound-Gaussian distribution based clutter models to fit the empirical PDF and calculated their distance with the proposed method, respectively. The result shows all models are approximately fit well with the empirical PDF. Still, differences can be observed from the tail region and the magnified local portion. On the other hand, the D_Ms (distances) quantify the fit qualities more accurately and their message accords with the figure. It suggests that model 4 has the minimum distance and the best fit.

5. CONCLUSION

This paper describes a modified goodness-of-fit measurement for radar clutter amplitude probability density function. The proposed method has advantages over existing ones in many aspects.

The proposed method provides a symmetric measurement, which is approximately independent from empirical PDF parameters such as, the sample number, the histogram cell-size and the range of the PDF. It can be used to make comparison over GoFs with multiple data sets without identical empirical PDF parameters. In addition, the variance estimation of the measured distance is provided, which is mainly dependent on the sample data number. With this variance, we can assess the accuracy of GoF.

REFERENCES

1. Yueh, S. H., J. A. Kong, J. K. Jao, R. T. Shin, H. A. Zebker, T. Le Toan, and H. Ottl, "K-distribution and polarimetric terrain radar clutter," *Progress In Electromagnetics Research*, Vol. 3, 237–275, 1990.

2. Frery, A. C., H. J. Muller, C. C. F. Yanasse, and S. J. S. Sant'Anna, "A model for extremely heterogeneous clutter," *IEEE Transactions on Geoscience and Remote Sensing*, Vol. 35, No. 3, 648–659, 1997.

3. Tatarskii, V. I. and V. V. Tatarskii, "Statistical non-Gaussian model of sea surface with anisotropic spectrum for wave scattering theory. Part I," *Progress In Electromagnetics Research*, Vol. 22, 259–291, 1999.

4. Balleri, A. and A. Nehorai, "Maximum likelihood estimation for compound-Gaussian clutter with inverse gamma texture," *IEEE Transactions on Aerospace and Electronic Systems*, Vol. 43, No. 2, 775–779, 2007.

5. Younsi, A. and M. Nadour, "Performance of the adaptive normalized matched filter detection in compound-Gaussian clutter with inverse gamma texture model," *Progress In Electromagnetics Research B*, Vol. 32, 21–38, 2011.

6. Habib, M. A., M. Barkat, B. Aissa, and T. A. Denidni, "Ca-Cfar detection performance of radar targets embedded in "non centered Chi-2 Gamma" clutter," *Progress In Electromagnetics Research*, Vol. 88, 135–148, 2008.

7. Farshchian, M. and F. L. Posner, "The pareto distribution for low

grazing angle and high resolution X-band sea clutter," *2010 IEEE Radar Conference*, 789–793, 2010.

8. Carretero-Moya, J., J. Gismero-Menoyo, A. Blanco-del-Campo, and A. Asensio-Lopez, "Statistical analysis of a high-resolution sea-clutter database," *IEEE Transactions on Geoscience and Remote Sensing*, Vol. 48, No. 4, 2024–2037, 2010.

9. Li, H. C., W. Hong, Y. R. Wu, and P. Z. Fan, "An efficient and flexible statistical model based on generalized Gamma distribution for amplitude SAR images," *IEEE Transactions on Geoscience and Remote Sensing*, Vol. 48, No. 6, 2711–2722, 2010.

10. Balleri, A. and A. Nehorai, "Maximum likelihood estimation for compound-Gaussian clutter with inverse gamma texture," *IEEE Transactions on Aerospace and Electronic Systems*, Vol. 43, No. 2, 775–779, 2007.

11. Owolawi, P. A., "Rainfall rate probability density evaluation and mapping for the estimation of rain attenuation in South Africa and surrounding islands," *Progress In Electromagnetics Research*, Vol. 112, 155–181, 2011.

12. Kanellopoulos, J. D., A. D. Panagopoulos, and S. N. Livieratos, "Differential rain attenuation statistics including an accurate estimation of the effective slant path lengths," *Progress In Electromagnetics Research*, Vol. 28, 97–120, 2000.

13. Anastassopoulos, V., G. Lampropoulos, A. Drosopoulos, and M. Rey, "High resolution radar clutter statistics," *IEEE Transactions on Aerospace and Electronic Systems*, Vol. 35, No. 1, 43–60, 1999.

14. Sokal, R. R. and F. J. Rohlf, *Biometry: The Principles and Practice of Statistics in Biological Research*, Freeman, New York, 1981.

15. Meyer, M. E. and D. V. Gokhale, "Kullback-Leibler information measure for studying convergence rates of densities and distributions," *IEEE Transactions on Information Theory*, Vol. 39, No. 4, 1401–1404, 1993.

16. Koehler, K. J. and K. Larntz, "An empirical investigation of goodness-of-fit statistics for sparse multinomials," *Journal of the American Statistical Association*, Vol. 75, No. 370. 336–344, 1980.

17. Scott, D. W., "On optimal and data-based histograms," *Biometrika*, Vol. 66, No. 3, 605–610, 1979.

18. *NIST/SEMATECH e-Handbook of Statistical Methods*, http://www.itl.nist.gov/div898/handbook/.

19. Cha, S., "Comprehensive survey on distance/similarity measures

between probability density functions," *International Journal of Mathematical Models and Methods in Applied Sciences*, Vol. 1, No. 4. 300–307, 2007.

20. Bar-Lev, S. K. and P. Enis, "On the classical choice of variance stabilizing transformations and an application for a Poisson variate," *Biometrika*, Vol. 75, No. 4, 803–804, 1988.

21. Guan, Y., "Variance stabilizing transformations of poisson, binomial and negative binomial distributions," *Statistics and Probability Letters*, Vol. 79, No. 14, 1621–1629, 2009.

22. Chernoff, H. and E. L. Lehmann, "The use of maximum likelihood estimates in χ^2 tests for goodness-of-fit," *The Annals of Mathematical Statistics*, Vol. 25, No. 3, 579–586, 1954.

23. Farina, A., F. Gini, M. V. Greco, and L. Verrazzani, "High resolution sea clutter data: Statistical analysis of recorded live data," *IEE Proceedings — Radar, Sonar and Navigation*, Vol. 144, No. 3, 121-130, Jun. 1997.

24. Arikan, F., "Statistics of simulated ocean clutter," *Journal of Electromagnetic Waves and Applications*, Vol. 12, No. 4, 499–526, 1998.

25. Li, L., L. Kong, and X. Yang, "A new amplitude probability density function estimation method for IPIX Grimsby data," *IEEE CIE International Conference on Radar*, Vol. 2, 1288–1290, 2011.